VIII ECCOMAS Thematic Conference on Smart Structures and Materials
SMART 2017
A. Güemes, A. Benjeddou , J. Rodellar and Jinsong Leng (Eds)

THERMAL AND MECHANICAL PROPERTIES OF SELF-HEALING EPOXY/GRAPHENE NANOCOMPOSITES

I. AGUIRRE DE CÁRCER *, M.G. PROLONGO*, C. SALOM*, J. PARRADO*, R. MORICHE AND S.G. PROLONGO†

* Dpt. Materiales y Producción Aeroespacial, Universidad Politécnica de Madrid, Spain.
e-mail: mg.prolongo@upm.es, catalina.salom@upm.es
†Dpt. Ciencia e Ingeniería de Materiales, Universidad Rey Juan Carlos, Madrid, Spain
e-mail: silvia.gonzalez@urjc.es

Key words: self-healing epoxy, graphene, thermal-mechanical-electrical properties.

Abstract. The goal of the present work is to analyze the influence of the type of graphene and graphene content on the thermo-mechanical properties of an epoxy nanocomposite formed by an epoxy resin base on diglycidyl ether of bisphenol A (DGEBA) and 4-aminophenyl disulphide (AFD) as curing agent. This is a "dynamic" epoxy matrix (vitrimer), which has reversible crosslinks based on aromatic disulphide bonds. The idea is to take the advantage of the high thermal conductivity of graphene nanocomposites to promote the self-healing. The study of the epoxy-graphene systems was carried out using two types of graphene: un-functionalized and a functionalized graphene. The functionalized graphene contains amine groups that are reactive with the epoxy prepolymer, forming nanocomposites in which the graphene nanoplatelets remain chemically anchored to the matrix. Dispersions of GNPs in the DGEBA were studied by Differential Scanning Calorimetry (DSC) in order to investigate the curing reaction. Dynamic Mechanical Thermal Analysis (DMTA) and tensile stress-strain measurements were performed to compare the glass transition temperature, the storage modulus in the glassy and rubber states, the Young modulus, deformation at break, mechanical strength and toughness. Electrical conductivity and combined tensile stress-electrical resistance experiments are reported for these nanocomposites.

1 INTRODUCTION

Recently it has been presented a new epoxy vitrimer [1] formed through the reaction of diglycidyl ether of bisphenol A (DGEBA) with 4-aminophenyl disulphide (AFD). This is a "dynamic" epoxy matrix, which has reversible crosslinks based on aromatic disulphide bonds. Vitrimers are new polymer networks that can be healable/repairable and recyclable. They can flow when reaching a given temperature, since the exchange reaction is initiated with temperature however they retain a fixed crosslinking density throughout the thermal processing, with covalent bonds in a constant exchange [2]. The new epoxy network DGEBA/AFD presents good mechanical properties, while showing reprocessability, reparability and recyclability [1]. Moreover it has exceptional characteristics compared to other vitrimers: 1) ease of synthesis from readily available materials, 2) fast stress relaxation at high temperature (vitrimer behaviour) without the need of a catalyst and 3) easy

applicability for the manufacture of (re) processable, repairable and recyclable FRPCs [1]. Recently we have studied the self-heating by the Joule effect in composites reinforced with CNTs and GNPs [3]. We confirm that Graphitic nanofillers induce an increase of the thermal conductivity of the epoxy resin, proportional to the nanofiller content and that the electrical conductivity has a clear percolation threshold. Electrical conductivity is needed to create the Joule Effect. In this work, we study the curing, thermo-mechanical and electrical properties of a self-heating epoxy (DGEBA-AFD) and their graphene nanocomposites. The idea is to take the advantage of the high thermal conductivity of grapheme nanocompoposites to promote the self-healing.

2 EXPERIMENTAL

2.1 Materials

An aeronautical grade epoxy prepolymer based on a basic DGEBA, Araldite LY556 (LY), was purchased from Huntsman. The curing agent: 4-aminophenyl disulfide (AFD) was purchased from TCI Europe. AFD was mixed at stoichiometric concentration with respect to oxirane rings. Moreover samples containing an excess of AFD (11% by weight) have been prepared.

The epoxy-graphene nanocomposites were prepared using two types of graphene with different nanoplatelet dimensions: GNPn was purchased from Cheap-Tubes (GNPS grade 4) and GNP_{M25} was purchased from XGScience. GNPn graphene nanoplatelets have average thickness < 4 nm and an average lateral size of 1-2μm, and GNP_{M25} graphene nanoplatelets have average thickness of 6-8 nm and an average lateral size of 25 μm. Frekote from Loctite was employed as mold release product.

2.2 Preparation of the dispersions and nanocomposites

Dispersions of graphene nanoplatelets in the epoxy prepolymer were obtained through sonication during 60 min using a horn and a sonicator UP400S Hielscher: 0.5 s cycles with a power of 400 W and amplitude of 50%. The temperature did not exceed 80°C. Dispersions were prepared with 1wt%, 4wt% and 6wt% of GNPs. Once the dispersions were obtained, the curing agent (AFD) was added at 80-85 °C and mixed during 5 min, these samples were studied by differential scanning calorimetry (DSC) in order to investigate the curing reaction.

Moreover specimens for dynamic mechanical thermal analysis (DMTA) and for tensile tests were prepared. For this purpose after adding the AFD to the dispersions they were degased under vacuum (15 min, 50 mmHg) and poured in aluminum molds of suitable dimensions and cured in an oven following the protocol: 8h at 140 ºC under atmospheric pressure. The molds were coated with a release product.

AFD /LY ratio was stoichiometric (molar ratio amino hydrogen / epoxy group = 1.00). There have been also prepared samples having (11wt% excess of AFD) in order to compere results of the neat system with the previously reported [1]

2.3 Techniques

Differential Scanning Calorimetry (DSC): a Mettler Toledo mod.822e differential scanning calorimeter was used. The instrument was calibrated with indium and zinc. Measurements

were performed under a nitrogen atmosphere Samples of 10-20 mg were weighted in aluminum pans. The reaction enthalpy (ΔH) and the exothermic peak temperature (T_p) were obtained from the first scans (-50ºC to 270ºC) of the reactive mixtures and dispersions. For each composition several first scans were done at different heating rates from 3 to 10 °C·min^{-1} in order to calculate the apparent activation energy of the curing reaction (E_a). To obtain the T_g of the nanocomposites samples were scanned from 25 ºC to 250 ºC at 10ºCmin$^{-1.}$ The T_gs were taken at the midpoint of the heat capacity change.

Dynamic Mechanical Thermal Analysis (DMTA): a DMTA V Rheometric Scientific instrument was used. Measurements of cured samples were performed in dual cantilever bending mode at 1, 2, 5, 10 and 50 Hz, with temperature increasing from 30 °C to 220 °C at a heating rate of 2 °C·min^{-1}. Specimens dimensions were: 35×10×1.8 mm^3. The elastic or storage modulus ($E´$), the loss modulus ($E´´$) and loss tangent ($tan\delta$) were recorded for each frequency as a function of temperature. The maxima in $tan\delta$-temperature curves were determined to identify the α-relaxations associated to the glass transitions.

Tensile tests: a MTS machine model QTest 2L with a load cell of 2 kN, using an MTS extensometer model 63411F-54 was used to study tensile mechanical properties of the nanocomposites. Experiments were performed at room temperature (22 ºC) at constant speed of 1 mm· min^{-1} until fracture. The specimen dimensions were 140 x10 x 1.8 mm^3. The stress-strain curves were recorded for six samples of each composition. The average values of mechanical properties: tensile modulus, tensile strength, strain to failure were calculated for each composition. Mechanical tests with the simultaneous measurement of the electrical resistance were performed using a Zwick Roell 100 kN machine with a coupled load cell of 5 kN and a meter instrument Agilent 34410A.

DC volume electrical conductivity was measured according to ASTM D257 using a Source Meter Unit instrument (Keithley 2410). The electrical resistance was determined from the slope of the current-voltage curve, and the electrical conductivity taking into account the geometry of specimens (10 x 10 x 1 mm^3). Six samples of 6%GNPn nanocomposite were measured in the range of 0-15 V.

3 RESULTS AND DISCUSSION

3.1 Curing of GNP/epoxy dispersions by DSC

The thermograms of neat epoxy (LY-AFD) and 4wt% GNP_n/epoxy dispersion are shown in Figure 1.The exothermic peak corresponds to the epoxy-amine curing reaction. Table 1 shows the DSC results for neat LY-AFD mixtures having stoichiometric ratio and 11wt% excess of AFD, together with the results for the corresponding GNP_n and GNP_{M25} dispersions in LY-AFD, at different heating rates (v). As it was expected T_{peak} increases with increasing heating rate, this is because faster heating rates offer less time for reaction, and to compensate for the reduced time the curves shift to a higher temperatures. $-\Delta H$ for each composition slightly decreases as the heating rate increases, but the variation is almost within the experimental error. Moreover there are not significant changes of $-\Delta H$ adding excess of AFD neither in the presence of 1% and 4% of GNP, indicating that all the epoxy groups in the LY-AFD mixture have reacted.

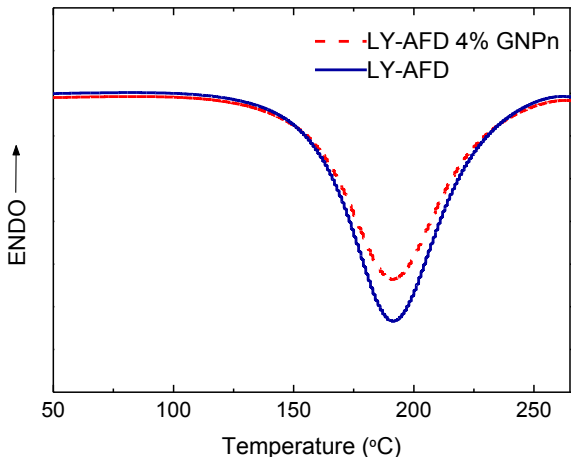

Figure 1: DSC thermograms (10ºC/min) of epoxy (LY-AFD) and 4wt% GNP_n/epoxy

Table 1: DSC results of curing epoxy (LY-AFD) and GNP/epoxy dispersions

	v (ºC/min)	***-ΔH*** (kJ/gLY)*	T_{peak} (ºC) †	T_g (ºC) ††	***Ea*** (kJ/mol)
LY-AFD	3	583	162	122	64±1
	4	574	169	128	
	5	564	175	131	
	8	550	187	136	
	10	524	193	136	
LY-AFD +1%GNP_n	3	578	160	124	62±1
	4	544	167	129	
	5	528	173	130	
	8	529	186	136	
	10	514	193	136	
LY-AFD + 4%GNP_n	10	530	192	137	-
LY-AFD + 4%GNP_{M25}	10	556	192	138	-
LY-AFD (11% excess)	3	568	159	113	62±0.5
	4	559	166	118	
	5	574	172	120	
	8	555	185	124	
	10	551	191	129	
LY-AFD (11% excess) + 4% GNP_n	10	558	191	130	-

Estimated error: * ±20 kJ/g, † ±0.5ºC, †† ±0.5ºC.

T_{peak} of samples containing 4% of GNP_n and 4% of GNP_{M25} is slightly lower than T_{peak} of LY-AFD (see Table 1) this reflects a small catalytic effect of GNP. However, no catalytic effect was noticed for samples containing lower GNP content, a previous work with another epoxy resin having 1% of GNP_{M25} showed similar behaviour [4]. The values of T_{peak} of LY-AFD (11% excess) are lower than the corresponding to LY-AFD which is due to the faster reaction of primary amine with respect to secondary amine. From the slope of the plots ln v vs. T_{peak}^{-1}, according to Arrhenius equation, the apparent activation energy of the curing reaction (E_a) was obtained and the results are given in Table1. A decrease of E_a is clearly detected of LY-AFD (11% excess) confirming that with amine excess the reaction goes faster.

The T_g values of samples cured during the first DSC scan are given in Table 1. The networks having excess of AFD have lower T_g than the stoichiometric LY-AFD samples. The preferential reaction of primary amine leads to networks with higher molecular weight between crosslinks, which corresponds with lower degree of crosslinking, and lower T_g. Regarding the effect of graphene on T_g the presence of GNPs has little influence on the T_g of the epoxy network for samples dynamically cured in the DSC.

3.2 Thermo-mechanical properties of DMTA of GNP/epoxy nanocomposites

DMTA curves ($E´$-temperature and tanδ-temperature for neat LY-AFD thermoset and for LY-AFD-GNPs nanocomposites at 1 Hz are given in Figures 2a and 2b.

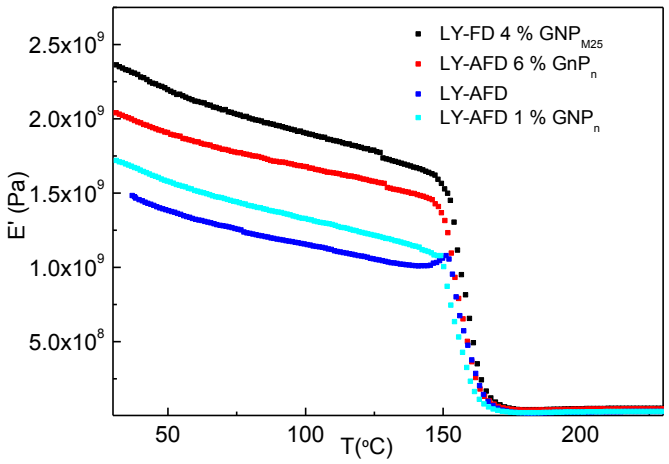

Figure 2a: $E´$-temperature of epoxy (LY-AFD) and epoxy/graphene nanocomposites

It can be see (Figure 2a) that in the glassy state ($T < T_g$) the nanocomposites have higher $E´$ than the neat epoxy thermoset. Table 2 collect $E´$ values for all the nanocomposites in the glassy and rubbery state ($T < T_g$). As it can be observed the addition of GNP increases the storage modulus in the glassy ($T < T_g$) and rubbery ($T > T_g$) states with regard to neat epoxy thermoset. The increment is proportional to the graphene content and is more important in the rubbery state. Moreover GNP_{M25} is a more effective reinforcement than the GNP_n as a consequence of its bigger size. The sample having AFD excess presents $E´$ *rubbery* lower than the stoichiometric (LY-AFD) which is due to its lower degree of crosslinking. The

opposite behavior is observed in the glassy state, because the stoichiometric network has all amine-epoxi bonds formed but is a less packed and more open network.

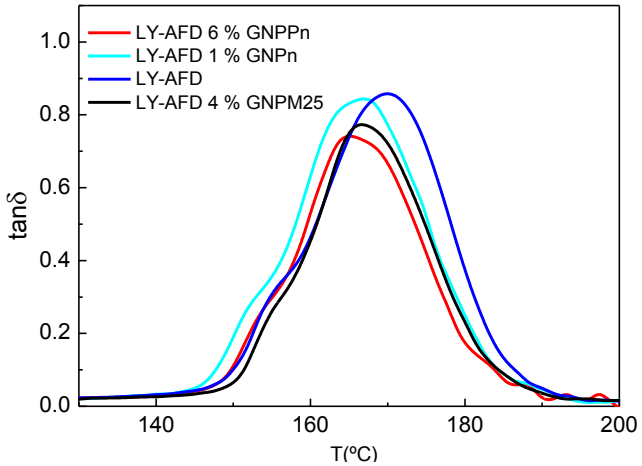

Figure 2b: *E´*-temperature of epoxy (LY-AFD) and epoxy/graphene nanocomposites

Table 2: *E´* modulus, temperature of $tan\delta_{max}$, of epoxy thermoset and GNP nanocomposites.

Sample	***E´glassy*** (80ºC) GPa	***E´rubbery*** (220ºC) MPa	***Ttan*δ_{max}** (ºC)
LY-AFD	1.23	28	170
LY-AFD (1% GNP_n)	1.41	29	167
LY-AFD (6% GNP_n)	1.75	47	165
LY-AFD (4% GNP_{M25})	2.00	50	166
LY-AFD(11% excess)*	1.35	27	168
LY-AFD(11% excess) + 4% GNP_n	1.54	33	162

*Curing: 2,5h -120ºC+ 2h-150ºC

It is noteworthy that the tanδ - temperature curves (Figure2b) show a main peak around 162ºC-170ºC and a shoulder at 12-15ºC below. This reflects that the epoxy matrix behaves mechanically as no homogeneous, that is, there are regions with high mobility that relax at lower temperatures and rigid regions that relax at higher temperature. This behaviour is minimized in networks cured with excess of AFD, where the tanδ - temperature curves show a single peak.

The temperature of $\tan\delta_{max}$ at 1 Hz (α-relaxation associated to the glass transition) for the neat epoxy thermoset and for the nanocomposites are included in Table 2. The T_g is taken as temperatura at which $\tan\delta$ (1Hz) reaches a máximum and usually T_gs from $\tan\delta_{max}$ (1Hz) are higher than the T_gs from DSC.The nanocomposites (see Table 2) have lower temperature of $\tan\delta_{max}$ than neat epoxy thermoset, i.e., a less perfect epoxy networks are formed in presence of GNPs.

3.3 Tensile properties of DMTA of GNP/epoxy nanocomposites

The tensile properties of nanocomposites were determined by tensile stress–strain measurements. Figure 3 shows the more representative stress–strain curves for epoxy thermosets and GNP nanocomposites. From the curves the values of tensile modulus *E*, tensile strength (stress at break), strain at break and area under stress-strain curves which is a measure of the toughness were calculated. Tensile test results are given in Table 3. The tensile modulus of the nanocomposites is higher than that of the epoxy thermoset evidencing the reinforcing action of the GNPs. The tensile strength, deformation at break and toughness values hardly changes with low GNP content (1%). However tensile strength, deformation at break and toughness decrease for 4% and 6% of GNP nanocomposites. This suggests the presence of defects in these nanocomposites.

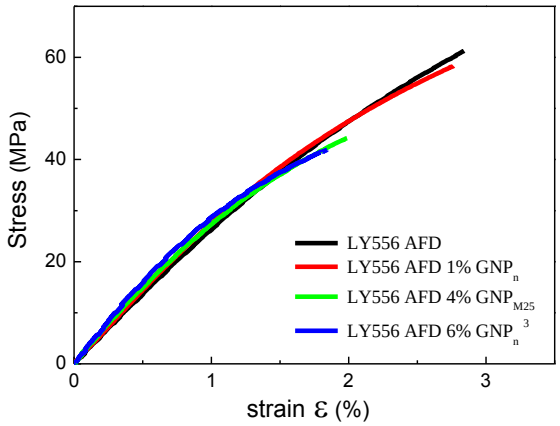

Figure 3: Stress–strain curves for epoxy (LY-AFD) and epoxy/graphene nanocomposites

Table 3: Stress-strain results for epoxy thermosets and GNP nanocomposites

Sample	**Young Modulus** (GPa)	**Tensile strength** (MPa)	**Deformacion at break** (%)	**Toughness** (MJ/m^3)
LY-AFD	2.76 ± 0.09	60± 4	2,8 ± 0.3	0.97
LY-AFD 1%GNP_n	2.83 ± 0.07	56 ± 3	2.7 ± 0.2	0.93
LY-AFD 6%GNP_n	3.32 ± 0.19	42 ± 2	1.8 ± 0.3	0.46
LY-AFD 4%GNP_{M25}	3.21 ± 033	46 ± 4	2.1 ± 0.4	0.51

3.4 Combined tensile tests-electrical conductivity GNP/epoxy nanocomposites

It is known that in nanocomposites the electrical conductivity shows a percolation threshold, this means that at GNP contents lower than the percolation threshold, the composites are insulator but their electrical conductivity increases abruptly at higher contents. The electrical percolation depends on the connectivity between nanoplatelets. Previous works [3] have shown that for GNP_{M25}-epoxy nanocomposites the percolation threshold is close to 3%. As GNP_n has smaller dimensions, it is expected that its electrical percolation would be reached at higher GNP_n content. In order to select a suitable composition to carry out the combined tensile stress-electrical conductivity tests, we have determined the conductivity of nanocomposites. Figure 4 shows the Intensity-Voltage dependence for six samples of LY-AFD-6%GNP_n. From the slopes of Intensity-Voltage lines and considering the sample geometry, a value of $10.4 \cdot 10^{-5}$ $S \cdot m^{-1}$ was found, which is suitable for the combined tests.

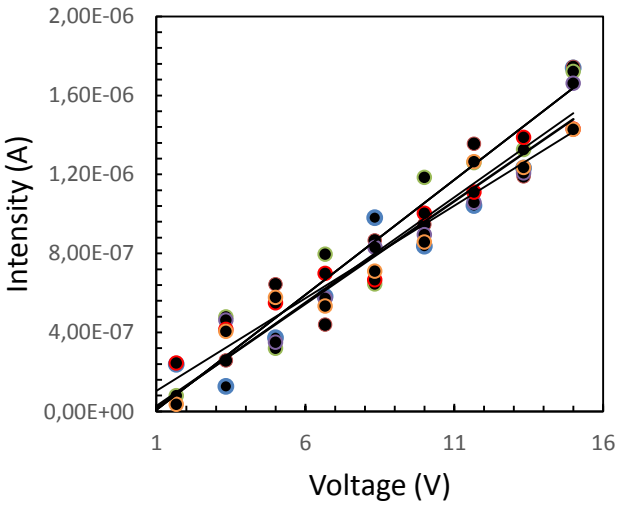

Figure 4: Intensity vs.-voltage for LY-AFD-6%GNP_n nanocomposites

In order to perform the combined tensile stress-electrical conductivity test of LY-XB-6%GNP_n nanocomposite, the specimens prepared for the tensile stress–strain test were painted around the perimeter with conductive silver paint at set intervals. Copper wire was then attached to the painting and covered with an adhesive thermoplastic, so efficient electrical contacts between the silver and the copper were produced. This set up creates five channels which allow the measurement of the electrical properties of the material at differentiated locations as can be seen in Figure 5 a. The tensile force-time curve of this set up was assayed at 5 mm/min while measuring simultaneously the two point electrical resistance at the different channels. The combined tensile force-electrical conductivity test for the LY-AFD-6%GNP_n specimen is shown in Figure 5 b. It can be seen the tensile force-time curve together the normalized resistance-time curves for the five different channels.
As the strain builds up in the specimen the electrical resistance through the different channels increases as seen by the rise in normalized resistance of all the channels. When the stress

disappears, in this case due to the specimen breaking, the conductivity of the channels returns to basal values, but the channel where the break occurs (chanel 11 in Figure 5) shows no conductivity after the break. This experiment would indicate that addition of 6% of graphene is not adequate as electrical sensor in the experimental conditions (high strain rate). Nevertheless this result suggest that reducing strain rate and/or GNP_n content, GNP_n could be used as electrical sensor.

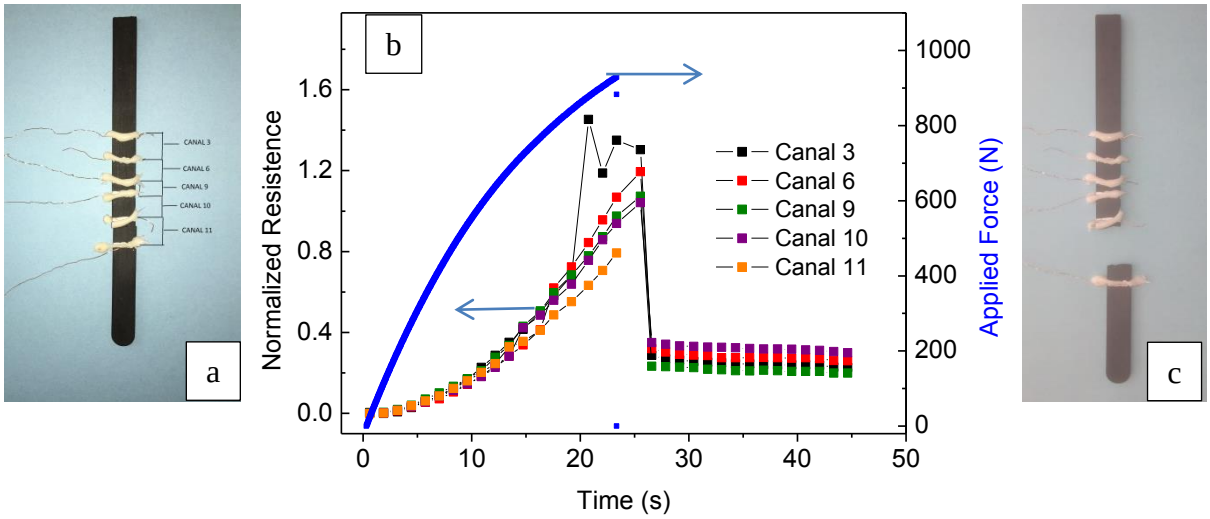

Figure 5: Combined tensile tests-electrical conductivity for LY-AFD-6%GNP_n nanocomposite: a)Specimen set up with five conductive channels before test, b) Force- time curve (—) together with resistance-time curves (□) measured in five channels, c) specimen after break.

4 CONCLUSIONS

- Incorporation of GNP up to 6% does not significantly modify the curing reaction of LY-AFD, nor in the presence of an excess of 11% of AFD.
- A small catalytic effect of GNP on curing LY-AFD was detected and the curing rate in excees of AFD (11%) is faster than in the stoichiometric LY-XB mixture.
- The networks having excess of AFD have lower T_g than the stoichiometric LY-AFD samples due to their higher molecular weight between crosslinks.
- The nanocomposites present increased glassy and rubbery moduli with regard to neat epoxy thermoset. The increment is proportional to the graphene content and is more important in the rubbery state.
- GNP_{M25} is a more effective reinforcement than the GNP_n as a consequence of its bigger size.

- The sample having AFD excess presents *E´ rubbery* lower than the stoichiometric (LY-AFD) due to its lower degree of crosslinking. The opposite behavior is observed in the glassy state, because is a more packed network.
- Increasing GNP content increases the tensile modulus at room temperature. Tensile strength, strain at break and toughness decrease with the increase of GNP content suggesting the presence of defects.
- The measured conductivity of LY-AFD-6%GNP_n is $10.4 \cdot 10^{-5}$ $S \cdot m^{-1}$ been suitable to carry out the combined tensile stress-electrical conductivity tests.
- The combined tensile force-electrical conductivity test for the LY-AFD-6%GNP_n specimen suggests that reducing strain rate and/or GNP_n content, GNP_n could be used as electrical sensor.

Acknoledgements

The authors acknowledge the financial support by Ministerio de Economía y Competitividad of Spain Government (Projects: MAT2013-46695-C3 y MAT2016-78825-C2)

REFERENCES

[1] Ruiz de Luzuriaga A., Martín R., N. Markaide, Rekondo A., Cabañero G., Rodríguez J. and Odriozola I. Epoxy resin with exchangeable disulfide crosslinksto obtain reprocessable, repairable and recyclable fiber-reinforced thermoset composites. *Mater. Horiz.* (2016) **3**:241-247.

[2] Azcune I. and Odriozola I. Aromatic disulfide crosslinks in polymer systems : selt-healing, reprocesability, recyclability and more.*Eur. Polym. J.* (2016) **84**:147-160.

[3] Prolongo S.G, Moriche R. Del Rosario G., Jiménez-Suárez A. Prolongo M.G. and Ureña A. Joule effect self-heating of epoxy composites reinforced with graphitic nanofillers. *J Polym Res* (2016) **23**:189 1-7

[4] Prolongo M.G., Salom C., Arribas C., Sánchez-Cabezudo M., Masegosa R.M., Prolongo S.G. Influence of graphene nanoplatelets on curing and mechanical properties of graphene/epoxy nanocomposites. *J Thermal Anal Calorim* (2016)**125**:629-636.